Pergamon

PII: S0191-8141(97)00106-5

Journal of Structural Geology, Vol. 20, No. 4, pp. 433 to 445, 1998

0191-8141/98 $19.00 + 0.00

Phyllonitization and development of kilometer-size extension gashes in a continental-scale strike-slip shear zone, north Goiás, central Brazil

J. F. HIPPERTT and A. J. MASSUCATTO

Departmento de Geologia, Universidade Federal de Ouro Preto, 35.400-000, Ouro Preto, MG, Brazil

(*Received* 28 *February* 1997; *accepted in revised form* 4 *November* 1997)

Abstract—Several km-scale, vertical extension gashes occur in a low metamorphic grade, strike-slip shear zone in central Brazil. These mega-gashes show many of the characteristics commonly found in en échelon extension gashes of cm and outcrop scale, reflecting a wide range of scale-invariance for this phenomenon. The gashes are filled with quartz veins which commonly host gold mineralization. Microstructures show a progressive deformation of the original cavity-infilling vein structures towards the gash margins. Logarithmic plots of length vs thickness for gashes from thin-section, outcrop and air photograph scales define a power law $L = 11.4\ T^{0.96}$. Logarithmic plots of cumulative frequency define curves with power-law segments whose slopes indicate 'fractal dimensions' D around 1.4–1.5 for both length and thickness. The phyllonite zones adjacent to the mega-gashes are interpreted to exert a crucial role in their development. Calculations show that the amount of quartz depleted in the phyllonite zones correspond to the amount of quartz precipitated in the mega-gashes ($\sim 7 \times 10^6\ m^3$). Volumes of fluid in the order of $10^{10}\ m^3$ must have been channelled through the opened fractures to precipitate such an amount of quartz. We conclude that these mega-gashes have developed from continuous propagation and opening of tension fractures in zones relatively preserved from phyllonitization (protomylonites). It is suggested that the development of kilometric extension gashes in the non-phyllonitic domains produces a volume gain in response to the volume loss produced in the phyllonite zones. The whole shear zone is envisaged, therefore, as an isovolumetric system with alternating lateral zones of volume loss (phyllonites) and volume gain (extension gashes). © 1998 Elsevier Science Ltd. All rights reserved

INTRODUCTION

This paper reports the occurrence of km-scale, vertical extension gashes formed during activation of the Cavalcante–Teresina strike-slip shear zone in north Goiás, central Brazil. These mega-gashes are completely filled with quartz veins up to hundreds of meters thick and show many of the recognizable geometrical and textural characteristics commonly described in extension gashes of cm and m scale (e.g. Hancock, 1972; Beach, 1975; Durney, 1981; Ramsay and Huber, 1987, p. 603; Rothery, 1988; Nicholson, 1991), reflecting a wide range of scale-invariance for this phenomenon. These common characteristics are: (1) development of an array with several subparallel veins; (2) individual extension veins generally oriented at 45° to the shear plane when observed in the plane XZ of finite strain; (3) presence of sigmoidal veins with a rotated central segment whose terminations are 45° oblique to the shear plane; (4) presence of cavity-infilling microstructures in the vein material; and (5) evidence for superimposed deformation in both veins and host rocks. We therefore believe that these gashes represent a superb natural laboratory to study the processes responsible for gash fractures and vein infilling in a simple shear kinematic framework. Apart from this, the kilometric dimensions of the infilling quartz veins reflect an extreme fluid influx and silica mobility in this shear zone. These gash veins are also an important prospecting target in the region as they host an unusual style of sulfide-free gold mineralization associated with palladium and platinum (Massucatto and Hippertt, 1996). In this paper, we present a description and a brief discussion concerning the development of these spectacular structures.

STRUCTURAL SETTING

The Cavalcante–Teresina strike-slip shear zone (Fonseca and Dardenne, 1993) is one among the many continental-scale, strike-slip movement zones that characteristically appear in the root of the Brazilian–Pan-African orogenic belts (600 Ma) of the Brazilian shield. The profusion of these strike-slip movements is a result of continental collision during the development of the Brazilian–Pan-African mobile belts (Vauchez *et al.*, 1995). The Cavalcante–Teresina shear zone appears in air photographs and Landsat images as a well-defined lineament oriented N40–60E in the northwest margin of the São Francisco craton. This shear zone extends from the Pirineus inflection (a domain of convergence of major strike-slip fault zones in central Brazil), and appears to continue for more than 1000 km to the northeast, beneath the Phanerozoic sequences of the Parnaíba basin. The Cavalcante–Teresina shear zone probably connects with the Senador Pompeu shear zone (Caby and Arthaud, 1986; Caby *et al.*, 1991) in northeast Brazil (Fig. 1). This paper is focused on the segment of the shear zone in the Cavalcante region (north Goiás), where the km-scale gashes occur (Fig. 2).

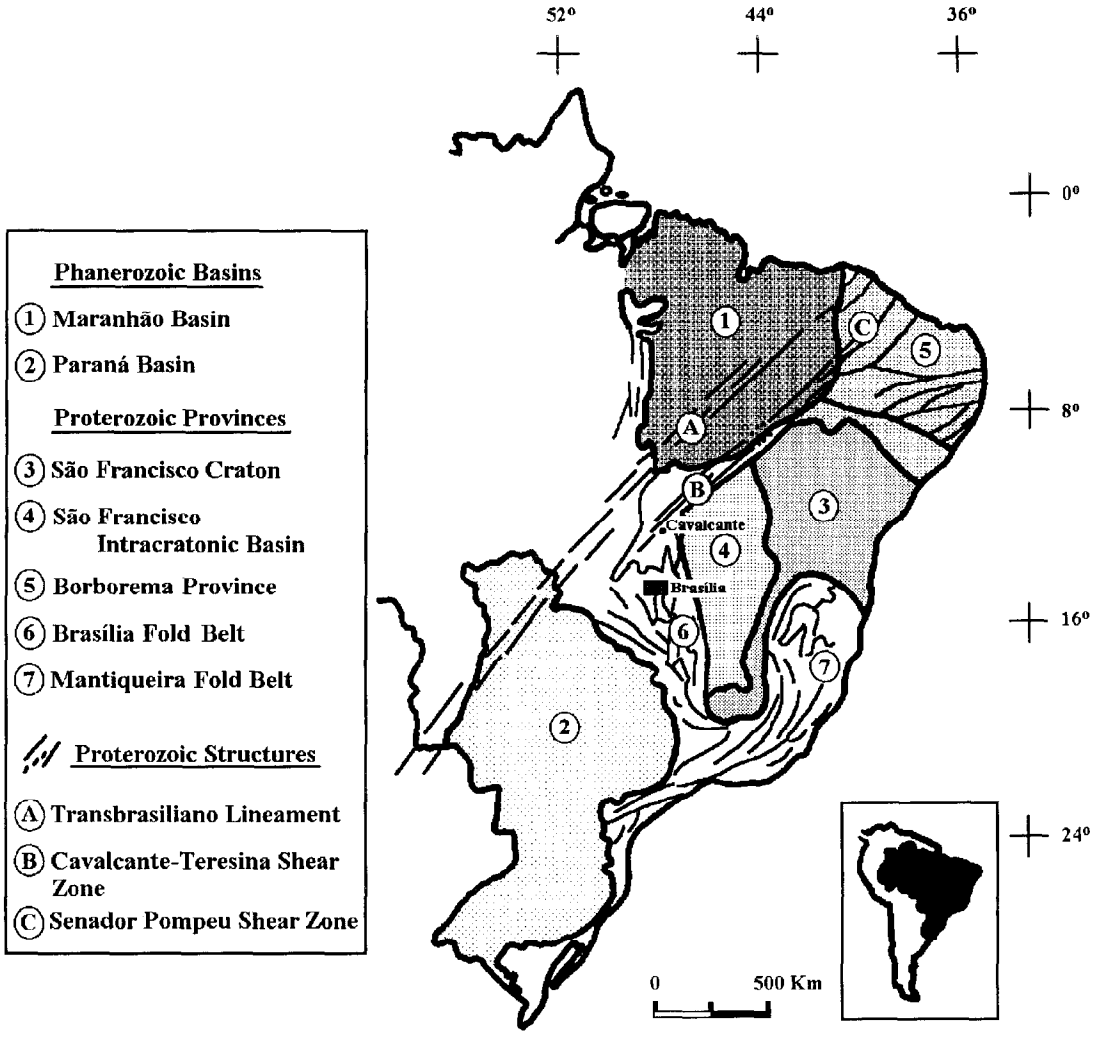

Fig. 1. Simplified geological map of east Brazil showing the major Phanerozoic and Proterozoic provinces.

In the Cavalcante region, the sheared granitic rocks of the Cavalcante–Teresina shear zone appear in an erosive window through the Proterozoic metasedimentary cover, which roughly follows the culmination of a 50 km wide antiform (Fig. 3). The sheared granitic rocks contain conspicuous vertical planar fabrics and a subhorizontal mineral stretching lineation defined by the morphological alignment of muscovite flakes. These vertical planar fabrics correspond to *S*- and *C*-foliations oriented at N10–30E and N40–60E, respectively.

Most strain in this shear zone was partitioned between two longitudinal domains, parallel to the shear zone margins, in which we observed an intense phyllonitization of the protolith granitic rocks. One of these domains (about 2 km wide) is adjacent to the southeast boundary of the shear zone. Another (about 8–10 km wide) occupies the central part of the shear zone (where the town of Cavalcante is located), and comprises several individual phyllonite zones varying in width from 200 m to 1 km, alternated with zones of intensely fractured protomylonitic rocks (Fig. 2). These two phyllonite domains are separated by a much less deformed domain (about 6 km wide) composed of protomylonitic rocks containing discrete (cm–dm scale) phyllonite zones. The *C*-foliations appear principally in the high strain, phyllonitic domains. In contrast, the *S*-foliation is widely predominant in the less deformed protomylonitic domains. The orientation of the *S*–*C* fabrics and other independent criteria consistently indicates a dextral sense of shear in this shear zone.

Deformation occurred under greenschist-facies conditions as indicated by strong development of phyllonites via mica-producing softening reactions, crystal-plastic deformation of quartz and brittle deformation of feldspars. However, in the less deformed domains, a relic higher temperature deformational fabric characterized by intense recrystallization of both quartz and feldspar is observed. The phyllonite zones may represent, therefore, a Brasiliano–Pan-African reactivation under shallower crustal conditions of a pre-existing Early or Middle Proterozoic movement zone. The km-scale extensional gashes that we describe below generally occur in the protomylonite domains situated between the individual phyllonite zones.

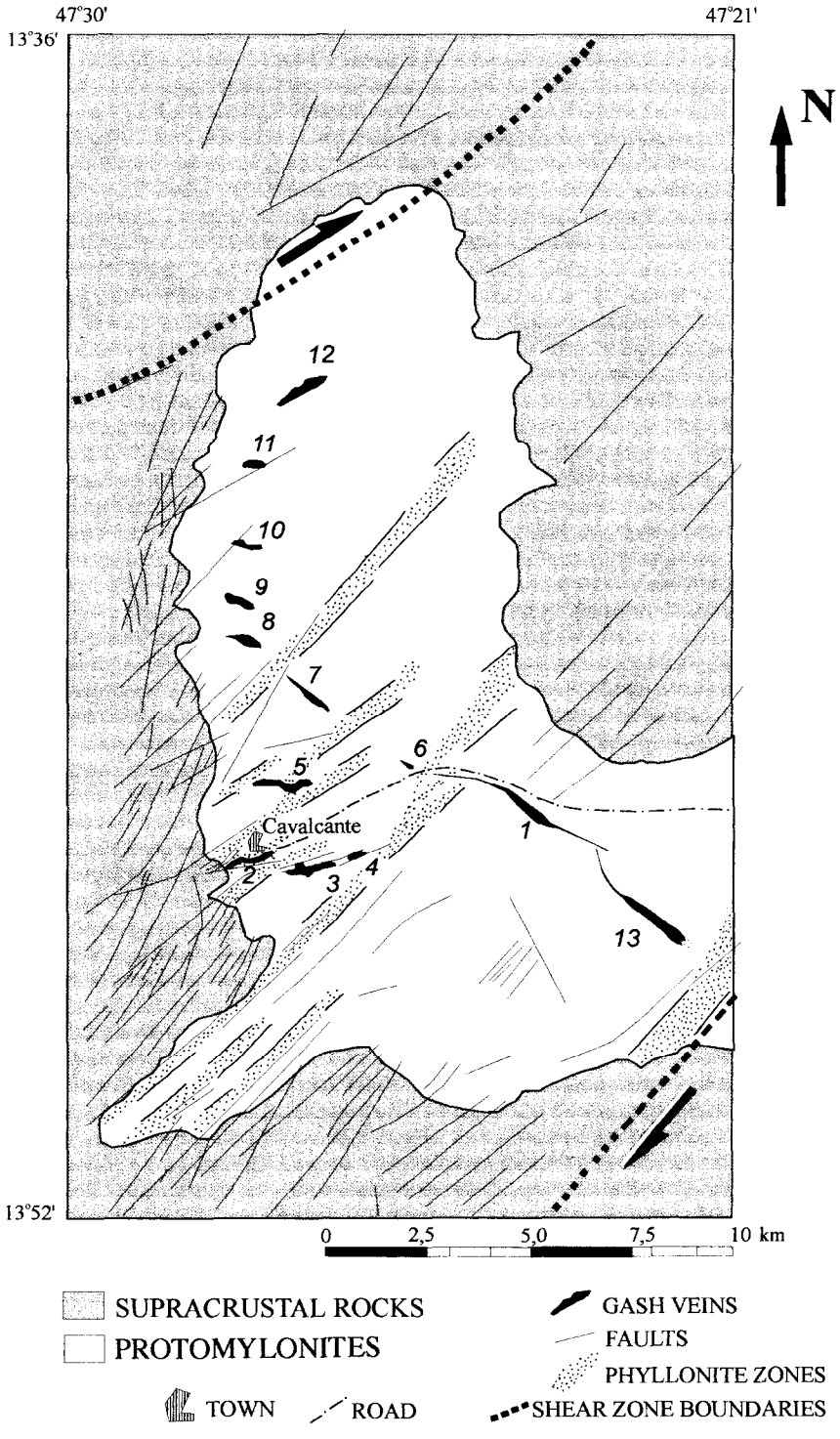

Fig. 2. Geological map of the strike-slip Cavalcante–Teresina shear zone, in the region of Cavalcante, Goiás, central Brazil. The gash veins (numbered 1–13) are hosted in deformed granitic rocks which are beneath a sequence of Proterozoic supracrustals (Araí group). The mylonitic rocks outcrop in a 20 km long erosive window (see also Figs 3 & 4a) which displays a transverse sector of the shear zone.

DESCRIPTION

Tectonites

Phyllonites and protomylonites are the main tectonite types in this shear zone. Typical mylonites and ultramylonites are only rarely found as discrete cm-wide zones in the middle of the protomylonite domains and will not be a focus of this description. Phyllonites and protomylonites occur in lateral zones of variable width (between cms and kms) which are generally parallel to the shear zone boundaries. A few phyllonite zones are oblique to the shear zone boundaries, and have the same orientation of the *S*-foliation (around

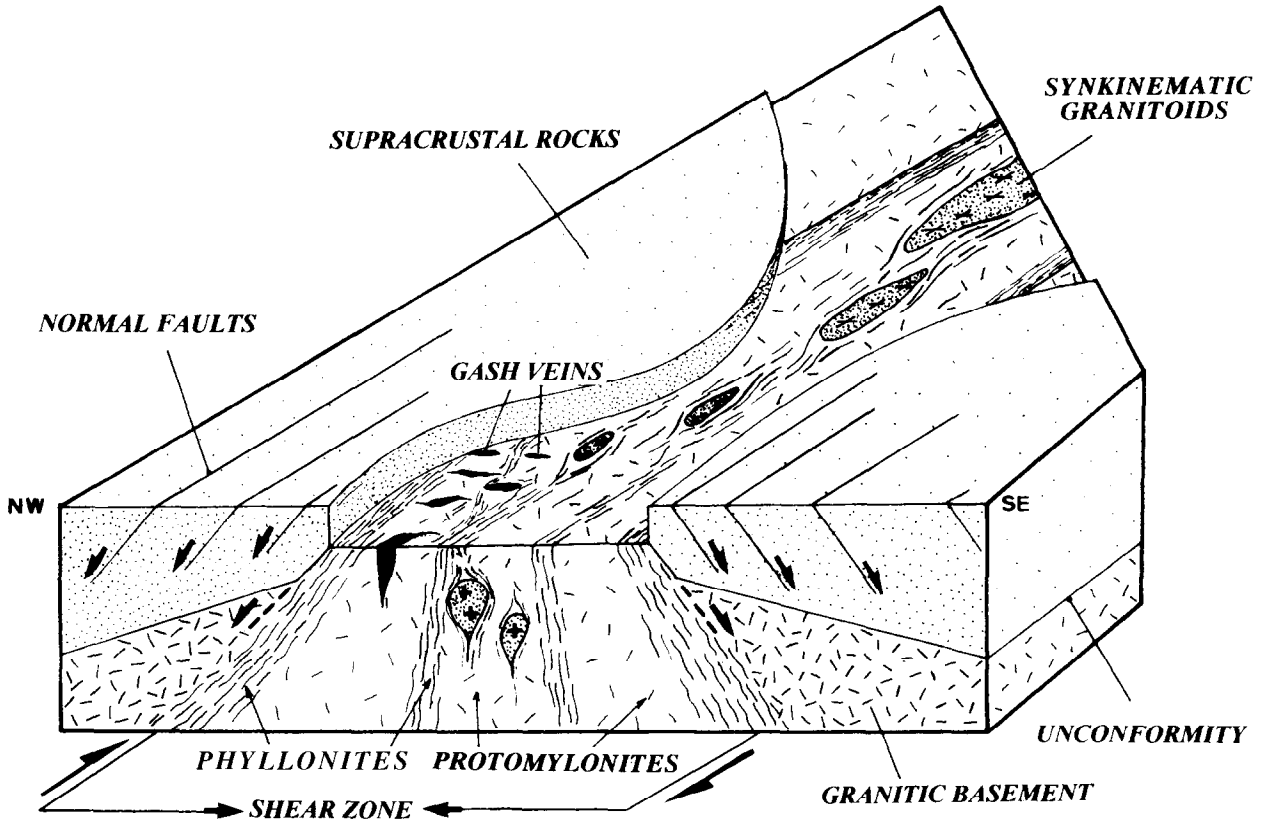

Fig. 3. Block diagram showing the structural setting of the strike-slip Cavalcante–Teresina shear zone, as well as their related synkinematic granitoids and vertical extension gashes. The frontal section is about 40 km long.

N20E). In their terminations, these phyllonite zones are progressively inflected towards the shear plane. The contact between phyllonite and protomylonite is generally transitional, and in places it is possible to observe over a distance of a few meters a complete lateral variation of microstructure, reflecting the progressive stages of phyllonitization of the protomylonite.

The protomylonite (Fig. 4a) is an isotropic or weakly foliated, coarse-grained rock conserving nearly the same modal composition of the protolith granitoid (plagioclase 38%, K-feldspar 29%, quartz 21%, biotite 10%), except for the minor amounts of muscovite associated with plagioclase breakdown in domains of incipient phyllonitization. This muscovite normally occurs along cleavages and fractures of plagioclase grains, where fluid access favored mica-producing softening reactions. Plagioclase is fractured and does not present any optically observable crystal-plastic deformation. K-feldspar is generally perthitic and displays no sign of chemical breakdown or crystal-plastic deformation. Quartz occurs as slightly elongate grains with strong undulating extinction and variable degrees of recrystallization along grain margins. Biotite shows incipient development of kinks and is generally partially transformed into muscovite along grain margins and basal cleavages.

The phyllonite zones generally correspond to well-defined lineaments on air photographs, because of their high mica content that causes their preferential weathering. The phyllonites (Fig. 4b) represent the extreme transformation of the original protolith within zones of high strain and fluid channelling within the Cavalcante–Teresina shear zone. They are composed of muscovite (75–60%), quartz (25–40%) and traces of opaque minerals. Small amounts of K-feldspar ($<$ 5%) may appear in some varieties where feldspar breakdown was not complete. Plagioclase is always absent. The muscovite is fine-grained (5–20 μm) and is preferentially oriented with basal planes parallel to the *C*-foliation. The longest dimension of the mica grains defines a well-marked stretching lineation. Quartz occurs as fine (5–10 μm), elongated grains intimately associated with muscovite, and also as large, undulating porphyroclasts (300 μm–2 mm) showing advanced stages of recrystallization and also fracturing and pull-apart (Fig. 4b). The recrystallized grains (40–150 μm) display a moderate crystallographic preferential orientation with a maximum parallel to the *Y*-axis of finite strain. This quartz *c*-axis fabric is interpreted to reflect the operation of prism $\langle a \rangle$ slip (e.g. Fueten *et al.*, 1991), one of the quartz slip systems that has its activation favored in the presence of water (Blacic, 1975).

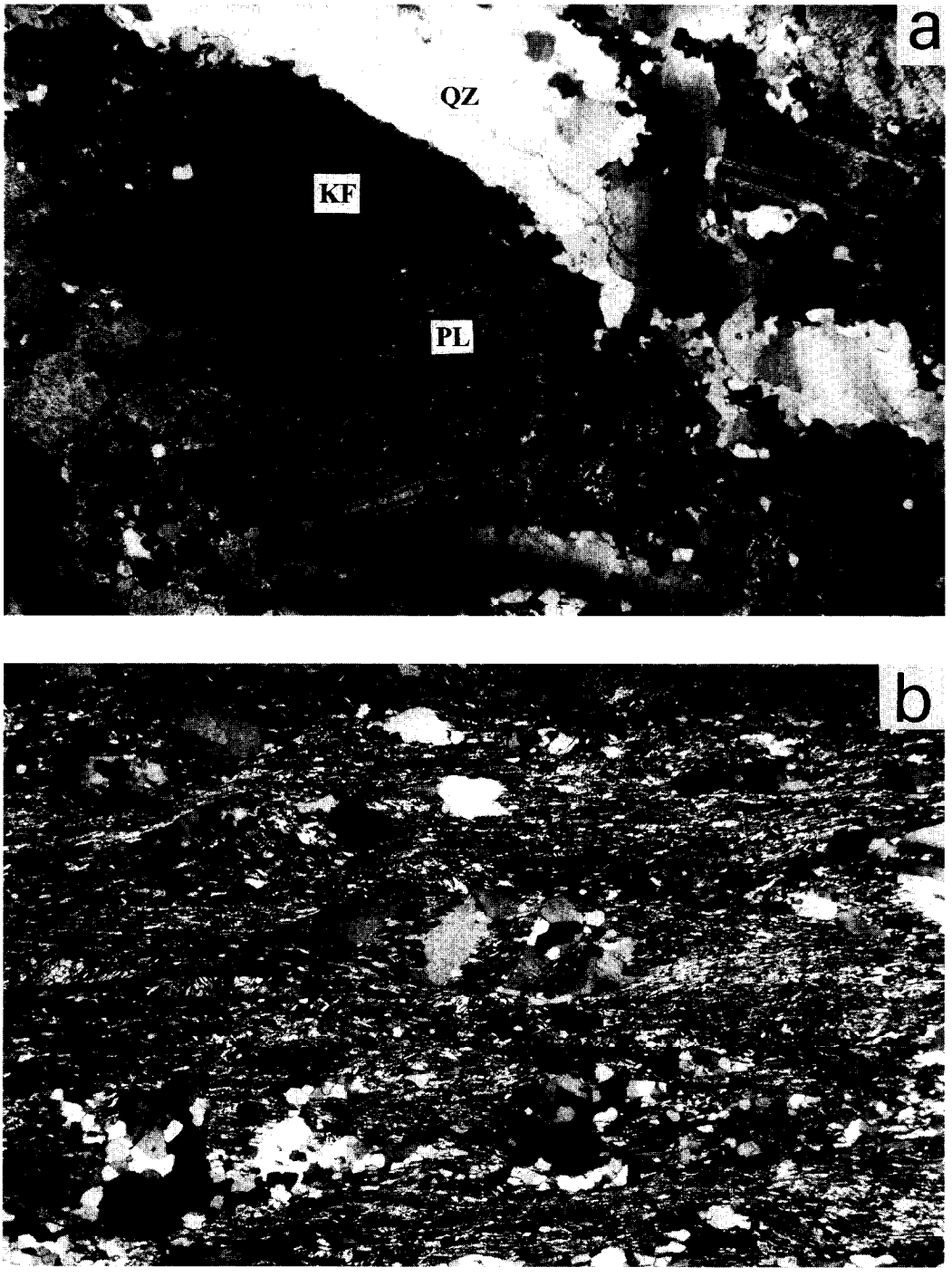

Fig. 4. (a) Typical protomylonite microstructure showing perthitic K-feldspar (KF) and fractured plagioclase grains (PL) partially transformed into muscovite along fractures. Quartz (QZ) shows undulose extinction, subgrains and partial recrystallization along grain margins. (b) Phyllonite microstructure showing partially recrystallized quartz porphyroclasts in a matrix of muscovite and fine-grained quartz. Note the fractures and pull-aparts in the large quartz porphyroclast in the center of the photograph. Photographs taken on *XZ* sections. Width of view 5.2 mm.

In contrast, fine-grained quartz associated with muscovite of the matrix shows a totally different preferential orientation with *c*-axes oriented at low angles to the stretching lineation. This fabric has been interpreted to form through direct precipitation from a fluid in low metamorphic grade tectonites where solution–reprecipitation creep has occurred (Tullis, 1989; Hippertt, 1994).

Gashes

Several km-scale gashes, here numbered from 1 to 13, occur within the protomylonitic domains in a radius of 15 km around the town of Cavalcante. These gashes are filled with quartz veins and have a noticeable topographic expression, appearing as abrupt ridges in the middle of a flat terrain of phyllonites and

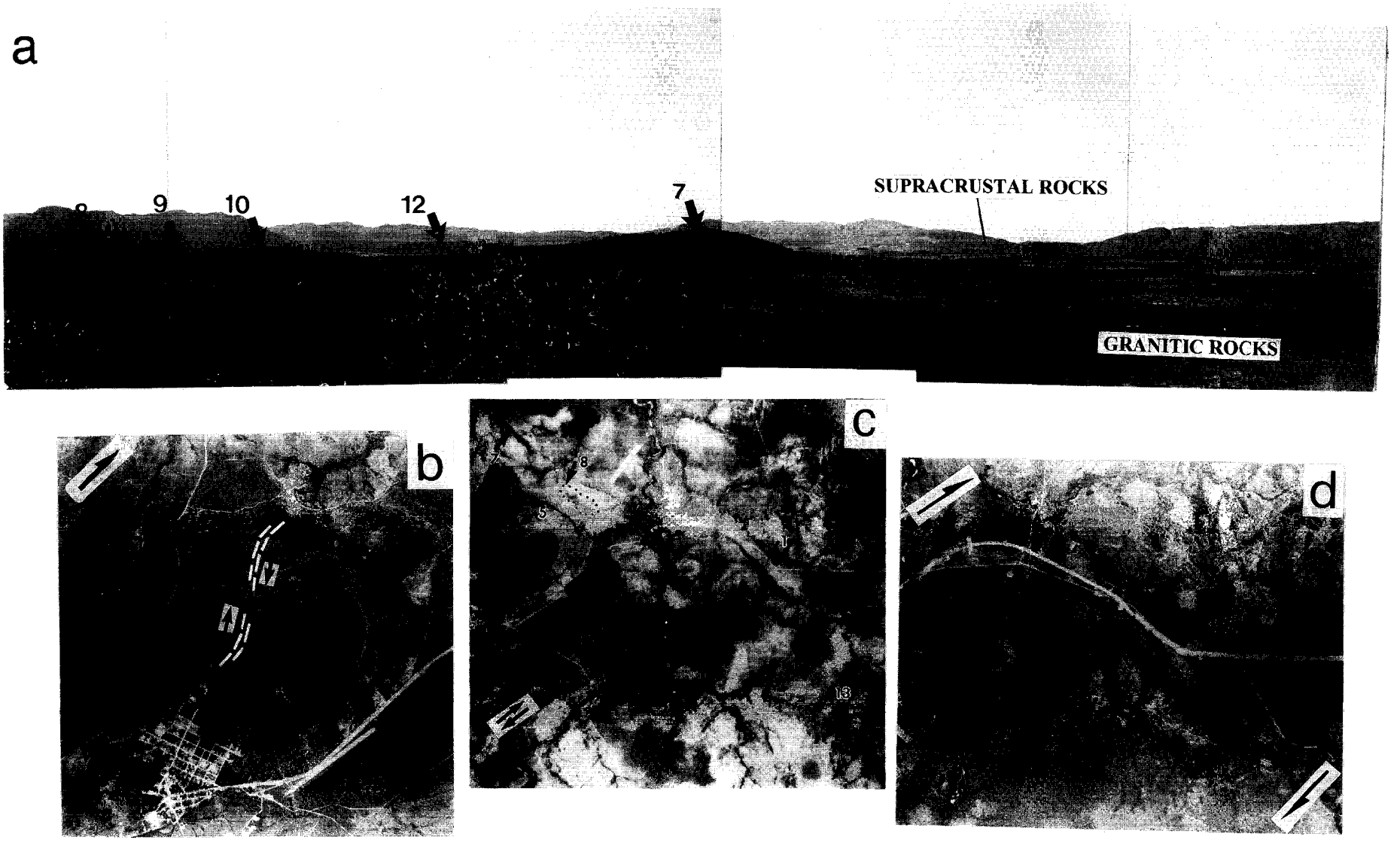

Fig. 5. (a) View of the north portion of the erosive window in the region of Cavalcante, showing gash veins 7, 8, 9, 10 and 12. This photograph was taken from gash 5 looking to the northeast (see Fig. 2 for location). Width of view is approximately 5 km. (b) Air photograph showing gash 5 which was displaced along a dextral phyllonite–mylonite zone (white dashed lines). The town of Cavalcante appears in the bottom of the photograph. Base of the photograph is 4.8 km. (c) Air photograph showing gashes 1 (sigmoidal), 5, 7, 8 and 13. Width of view is 10.5 km. (d) Detail of the sigmoidal gash 1. Width of view is 3.75 km.

protomylonites (Fig. 5a). On air photographs, i.e. a view parallel to the XZ plane of finite strain, the gash dimensions vary from 700 m to 4 km in length (measured in the Z-direction), with maximum thickness varying from 75 to 300 m (measured in the X-direction). Their apparent length/thickness ratio in air photographs varies from 4 to 22, with an average of 9.8. The gash walls are vertical or subvertical (dipping 80–85° to inside the gashes), but their dimensions in the vertical direction are not known. Underground prospecting surveys have traced the gash walls only to depths of 400 m. All gash veins display a lenticular shape in the horizontal plane. Most are linear, oriented at angles between 35° and 45° to the shear plane of the host tectonites. Gashes 8, 9 and 12 have different orientations (75°, 60° and 10°, respectively). The obliquity of all these gashes is consistent with an orientation at high angles to the maximum extension direction relative to the dextral shearing inferred from the S–C structures. Gash 1 is the only one that has a clear sigmoidal shape, also consistent with the geometry expected to form during dextral shearing (Fig. 5c & d). In this gash, the central part seems to have rotated synthetically with the superimposed shear. However, the gash terminations reflect the initial orientation of the extension fractures at angles close to 45° to the shear plane.

Zones of intense foliation development, mica enrichment and ductile deformation cross-cut most of the gashes. These zones normally correspond to topographic depressions in the gash profile because of the higher content of mica and preferential weathering. Gash 5 has been cross-cut and displaced by one of these zones. It is an 80 m wide, dextral shear zone with orientation corresponding to the regional S-planes (Fig. 5b). Most gashes terminate in phyllonite zones and there is no indication that the gash fractures continue through the phyllonites.

We have made transverse profiles and sampled the central part and terminations of all gashes. In the field, each gash consists of a single, apparently continuous quartz vein, which is composed of nearly pure, milky quartz in the central part, with increasing amount of muscovite (up to 10%) towards margins. On the hand-specimen and thin-section scale, there is a noticeable similarity between all the gash veins. One exception, however, is the sigmoidal gash 1 which underwent a more pervasive deformation which is reflected in the widespread occurrence of a fine-grained, recrystallized matrix.

Underground mining of gold in gash 2 has permitted detailed observation of the internal gash structure. No apparent lateral heterogeneities or evidence for multiple vein generation were found at outcrop scale. Evidence for sequential fracturing, cavity-infilling and syntaxial quartz growth is, however, present at a microscale. Figure 6 shows fractures oriented parallel to the gash walls in a thin-section from the central part of gash 2. The fracture in Fig. 6(a) is partially healed by large euhedral quartz grains (50–600 μm) nucleated in the fracture walls and grown with their c-axes tracking the separation trajectory. A totally healed fracture is shown in Fig. 6(b). These microstructures are found in the less deformed, central portion of most linear gashes, but not in the sigmoidal gash 1 where deformation was more pervasive. The fractures are irregularly spaced and are interpreted to represent the last stages of gash opening. Typical crack–sealing microstructures were not observed, indicating that the gashes opened at relatively fast rates, as also indicated by the presence of cavity-infilling microstructures (Nicholson, 1991). Towards the margins, however, obliteration of the cavity-infilling microstructures by the superimposed ductile deformation has produced aggregates of polygonal, recrystallized quartz grains (20–60 μm) with incipient crystallographic fabrics.

DISCUSSION

Phyllonitization and gash development

Superimposed deformation of the gash veins is observable even in those gashes where no apparent displacement or rotation can be seen. This deformation appears to have been continuously applied to the veins during their progressive crystallization, as the development of recrystallized polygonal aggregates increases towards vein margins. Other evidence for superimposed deformation comes from the presence of cross-cutting deformation zones that affect many of the gashes. Interestingly, these cross-cutting deformation zones always correspond to the orientation of the regional S-foliation (N10–30E) and never to the C-foliation (N40–60E) which appears in the limiting lineaments. We suggest that these cross-cutting deformation zones represent incipient phyllonite zones whose orientation corresponds to S-planes of a megascale S–C structure (Fig. 7) continuously formed during progressive deformation. The continued development of deformation zones (phyllonites) within the protomylonitic domains containing the mega-gashes suggests that the locus of movement could have shifted over time from one deformation zone to another within this 20 km wide shear zone.

This scenario with alternating zones of phyllonites and protomylonites reflects an extreme strain partitioning where most strain is accommodated via volume loss in the phyllonites (e.g. O'Hara, 1988; Selverstone *et al.*, 1991). It is likely that the silica depleted in the phyllonites was reprecipitated in the gash veins within the protomylonite zones. Indeed, the silica for this km-scale quartz veins may have been produced via large-scale feldspar breakdown and quartz removal associ-

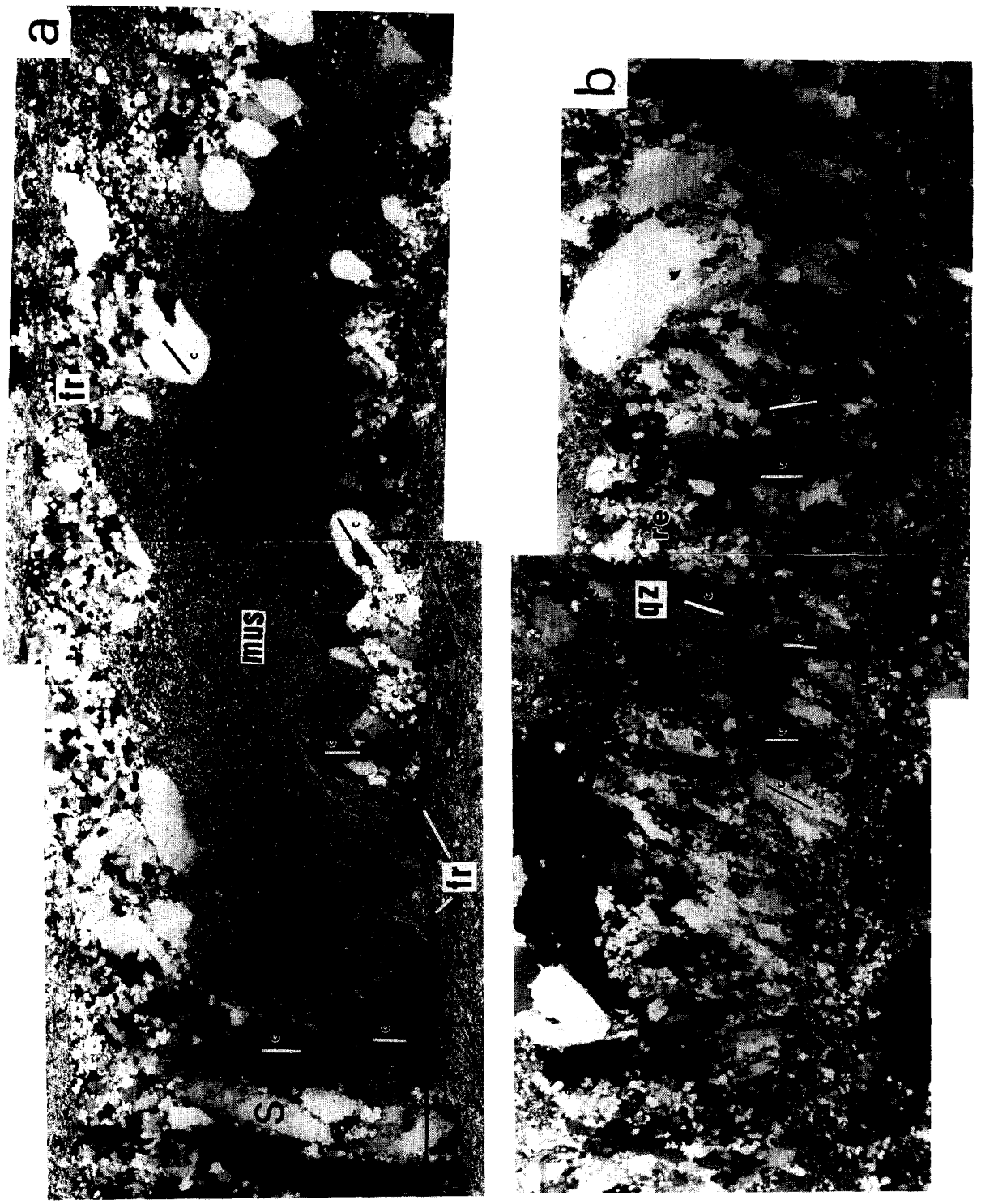

Fig. 6. (a) Partially healed fracture in the central portion of gash 2. The original fracture walls (fr) are oriented parallel to the gash margins. Quartz grains elongate parallel to [c] have nucleated in the fracture walls and grown towards the opposite wall. The *c*-axis trace is indicated in some grains. Note the totally sealed domain (S) on the left. The fracture space is filled with a fine-grained muscovite-rich aggregate (mus). Width of view is 10.8 mm. (b) Sealed microfracture affected by superimposed deformation–recrystallization in the marginal zone of gash 2. Note the undulose extinction in the original quartz grains (qz) grown with *c*-axis perpendicular to the fracture walls. These grains are surrounded by a matrix of fine-grained recrystallized quartz (re). Width of view is 10.8 mm.

ated with development of these up to 1 km wide phyllonite zones.

To check this hypothesis, we have estimated the silica depletion in the phyllonites by considering the changes in modal composition between the protolith granitoid and the resulting phyllonite, and the probable retrograde reactions involved in the process. The phyllonite zones occupy an area of about 20–25 km^2 on the map within the segment of the shear zone where the mega-gashes occur (Fig. 2). Previous studies of mass and volume changes based on chemical balance calculations have determined that mass and volume losses between 40 and 60% generally occur during phyllonitization of granitic protoliths (e.g. O'Hara, 1988; O'Hara and Blackburn, 1989; Selverstone *et al.*, 1991). Assuming 50% as a reasonable value of volume loss, we infer that a protolith area of 40–50 km^2 had to be affected to produce the observed phyllonite zones.

Phyllonitization of granitoids occurs mainly through breakdown of feldspars via mica-producing softening reactions. These reactions generally release alkalis and large amounts of SiO_2 (about 40 g per 100 g feldspar) to the fluid phase (O'Hara, 1988), that can account for the observed volume losses in phyllonites. In the Cavalcante–Teresina shear zone, the feldspar content in the protolith is around 70%. As nearly all feldspar has disappeared in the phyllonite, losses of SiO_2 corresponding to a volume of 11×10^6–13×10^6 m^3 per m of vertical section should have been produced as consequence of feldspar breakdown. Another possible way to produce volume loss in phyllonites is removal of the original quartz content (about 20%) through dissolution and mass transfer out of the phyllonite zone (Hippertt, 1994). The quartz content in these phyllonites varies between 25 and 40%. However, these contents of quartz are close to those expected to be produced by the simple residual concentration of the original quartz, considering a volume loss of 50%. We conclude, therefore, that quartz dissolution was a not a major mechanism during phyllonitization, and that all silica dissolved in the circulating fluid and precipitated in the mega-gashes originated through feldspar breakdown.

The mega-gashes occupy an area of about 12 km^2 on the map of Fig. 2. The average quartz content in the veins is 90%, corresponding to a volume of 10.8×10^6 m^3 per m of vertical section in the mega-gashes, which is well in accordance with the silica loss estimated for the phyllonite zones (11×10^6–13×10^6 m^3/m). These values, although derived from crude approximations, suggest that the entire shear zone possibly acted as a closed system for silica, where lateral migration of silica from the phyllonite zones towards the extension gashes may account for lateral compensation of volume between alternating zones of volume loss (phyllonites) and volume gain (extension gashes in the protomylonite zones) (Fig. 8). Mega-gashes and phyllonite zones, therefore, are interpreted as coupled, concurrent structures where the mega-gashes host the silica that was lost in the adjacent phyllonite zones.

Typically, gold–quartz veins are interpreted to document the passage of large volumes of aqueous fluid

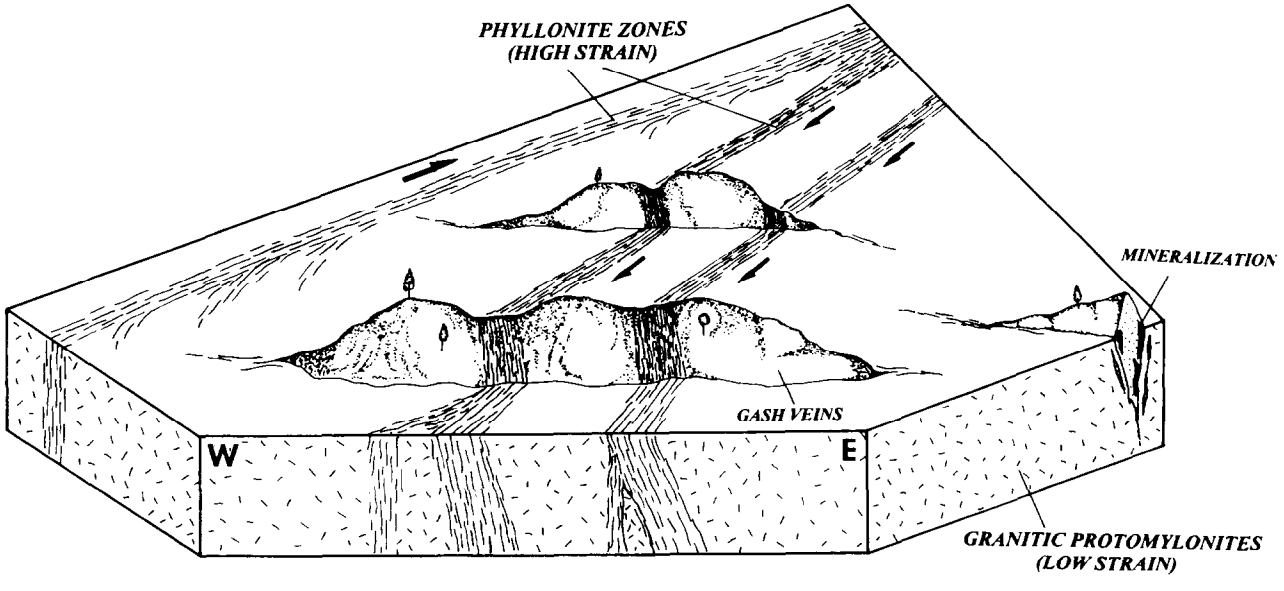

Fig. 7. Block diagram illustrating a three dimensional view of gash veins within the strike-slip Cavalcante–Teresina shear zone. The gashes have a noticeable geomorphological expression, appearing as abrupt ridges in a flat terrain comprised of deformed granitic rocks. Some gashes are cross-cut by oblique phyllonite zones, which generally correspond to depressions in the gash profile. Note that the geometry of the phyllonite zones seems to define a mega *S*–*C* structure consistent with the dextral shearing in the Cavalcante–Teresina shear zone. The gold mineralization that commonly occurs in the gash margins is also shown.

through fault-fracture networks (Cox *et al.*, 1991). If we estimate that the mega-gashes have a minimum length of 500 m vertically (as inferred from the underground mining), then the volume of quartz precipitated in these veins is at least 7×10^6 m^3. Considering the low solubility of silica (around 6 g SiO_2 per kg H_2O for low metamorphic grade conditions; Fournier & Potter, 1982), a minimum of 3×10^9 m^3 of aqueous fluid must have been flushed through the opening fractures to precipitated such a volume of quartz, assuming 100% efficient precipitation. Similar fluid volumes were also inferred for the 200 km long Mother Lode gold–quartz vein system of California (Sibson, 1994). Assuming that this volume of fluid channelled through the phyllonite zones had no dissolved silica, and estimating a minimum vertical length of 500 m for the phyllonite zones, we find a time integrated fluid/rock volume ratio for the phyllonites in the order of 10^2:1. However, if fluid was between 50 and 90% saturated in silica (a more likely scenario for fluid circulating through granitic rocks), fluid/rock ratios in the range 10^2–10^3:1 are found. These estimates are in good agreement with the results determined by O'Hara (1988) and Selverstone *et al.* (1991) in shear zones where phyllonitization of granitoids and volume loss took place.

As the gash walls dip at high angles inwards, we expect narrowing and closure of the veins downwards, i.e. along the *Y*-axis of finite strain (see Fig. 8). Analogy with the geometry shown by other documented gash veins (e.g. Johnston and McCaffrey, 1996) suggests that a dimension of 10–20 times the maximum thickness may occur along *Y*. Although extension gashes are natural low-pressure sinks for the fluid phase present in the deforming rock (J. Henderson, written communication 1997), they should also act as pathways for continued fluid circulation to allow formation of such km-scale quartz veins, considering the low solubility of silica. There is no indication of a connected vertical fracture network between the different gashes in the vertical, making fluid circulation through the gashes in this direction unlikely. In contrast, where two consecutive gashes are not separated by a phyllonite zone, there are some examples of connections in the *Z*-direction (e.g. gashes 1 and 13 in Fig. 2). This geometry suggests that the phyllonite zones should represent the main routes for fluid circulation, and that lateral circulation through the extension fractures may form a connected fluid circuit between two consecutive phyllonite zones (Fig. 9).

An important question concerns the fracture mechanisms involved in the formation of tension gashes. Assuming homogeneity of the deforming material and simple shear flow, gashes must have formed at 45° to the shear plane and developed as tension fractures parallel to the maximum principal stress σ_1 (e.g. Durney, 1981). In dilational shear zones, however, extensional failure at lower angles may also occur (Rickard and Rixon, 1983). In contrast, gashes at 15–20° to the shear plane have been commonly attributed to shear fracturing (e.g. Beach, 1975) and those at angles between 15° and 45° (as observed in the Cavalcante–Teresina shear zone) have been ascribed to a combination of these two fracture mechanisms (Hancock, 1985; Engelder, 1987). Apart from the obliquity of the gash tips, analysis of the internal fiber geometry is also crucial to elucidate the fracture mechanism involved during gash formation (Rickard and Rixon, 1983). In

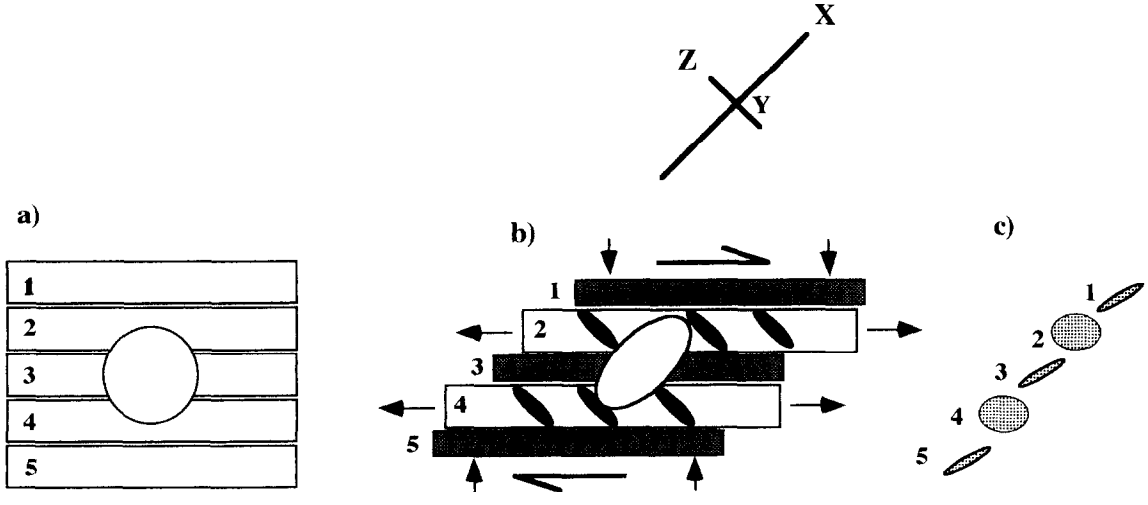

Fig. 8. Sketch illustrating strain partitioning and lateral compensation of volume between zones of phyllonites and protomylonites in the Cavalcante–Teresina shear zone. (a) Undeformed protolith. (b) Strain is heterogeneously accommodated in alternating zones of phyllonites (shaded) and protomylonites (white). Vertical arrows represent the contraction in the direction perpendicular to the shear plane caused by volume loss in the phyllonite zones. Horizontal arrows indicate the expansion in the shear plane (volume gain) due to development of extension gashes (black ellipses) in the protomylonite zones. The *XZ* bulk strain ellipse is indicated. (c) Distribution of the local *XZ* strain ellipses for the alternating zones of phyllonites and protomylonites (numbered 1–5).

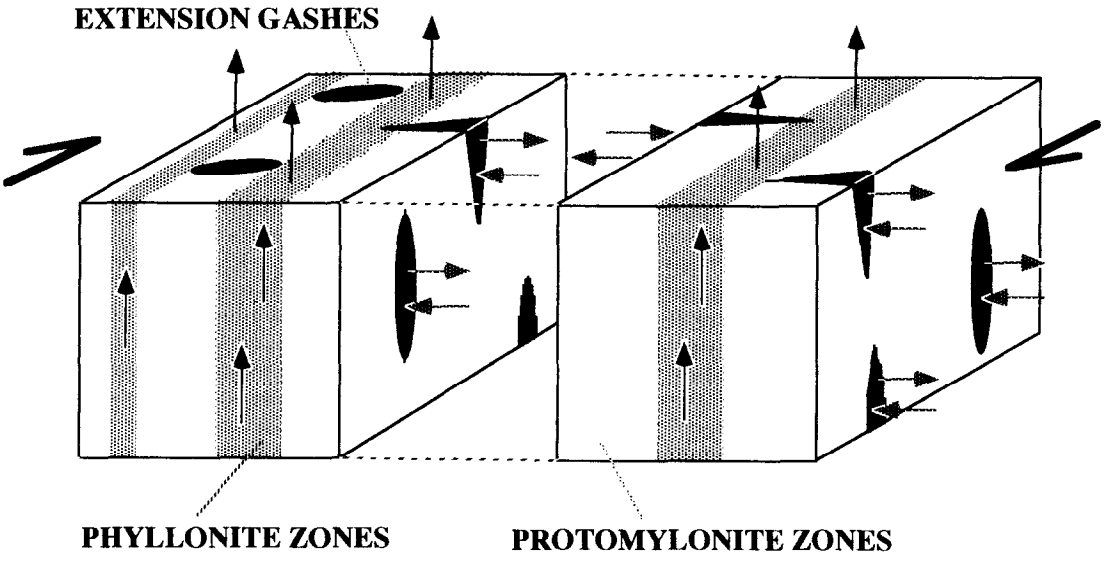

Fig. 9. Suggested pattern of fluid circulation in the Cavalcante–Teresina shear zone. Black arrows indicate the vertical fluid migration through the phyllonite zones with lateral fluid migration occurring through the extension gashes. Note how the extension gashes are not connected in the vertical direction.

the Cavalcante–Teresina shear zone, our observations of the internal fiber geometry in gash veins of mm–cm scale suggest participation of both extensional fracturing and shear fracturing components during gash formation as small mica flakes and thin quartz fibers, observable in thin sections, appear to track an oblique separation trajectory of the fracture walls.

Scale-invariance of extension gashes

Gashes of cm–m scale, showing the same composition and orientation as the mega-gashes, are also commonly observed in the Cavalcante–Teresina shear zone. An attempt was made to investigate the relationship between gash veins of different scales through measurements of thicknesses and lengths of gash veins from thin-section to air photograph scales. Figure 10(a) shows that gash veins on the micro-scale and outcrop scale plot in a straight line with the km-scale gashes in a logarithmic plot of length (L) vs thickness (T). This plot defines a power-law $L = K \cdot T^a$, where $K = 11.4$ and $a = 0.96$, with a goodness-of-fit $r > 99\%$. It should be noted that the dimensions of the mega-gashes, measured on air photographs, are sometimes difficult to determine because some gash boundaries are obscured by talus deposits. Thus, an overestimation of the gash thickness may be the reason for the deviation of some mega-gashes from the best-fit line in Fig. 10(a).

Similar power-law relationships between length and thickness have been demonstrated to occur in other vein systems with fractal characteristics (Johnston, 1992). The results in Fig. 10(a) are distributed over six orders of magnitude of size range. Even considering the small number of points in the graph, the exponent 'a' close to 1 suggests a self-similar distribution, where the same physical processes may have operated for development of gashes from micro- to km scale (Mandelbrot, 1985). However, a power-law data distribution should also be confirmed in diagrams of cumulative frequency. Logarithmic plots of cumulative frequency vs length and thickness for both outcrop and air photograph scales are shown in Fig. 10(b). These plots have defined curves with central power-law segments whose negative slopes indicate similar 'fractal dimensions' for length ($D = 1.38$–1.41) and thickness ($D = 1.51$–1.52) of the two gash populations. In this diagram, the database was split in two groups which were plotted separately, one with the mega-gashes and another with the outcrop and microscale gashes. This was necessary because the sampling is clearly non-uniform. The mega-gashes have a very representative sampling because virtually all existing gashes of km scale were measured. In contrast, the few data for gashes of outcrop and microscale are comparatively much less representative. This problem would necessarily lead to deviations of the power-law distribution in the curve terminations (Walsh and Watterson, 1992). The plot in two groups minimizes the problem, and the eventual fractal nature of the whole set can be assured by the same slopes of the straight segments of the curves of the two gash populations. In Fig. 10(b), it is also interesting to note the contrast in the resolution of the power-law segments between the two data populations. All mega-gashes plot with minimum deviations in a straight line because of their representative sampling. In contrast, the heterogeneous sampling in the outcrop scale has induced strong deviations in the curve terminations.

Our results contrast with those found in other power-law vein systems which have been generally interpreted as self-affine distributions (see Barton and

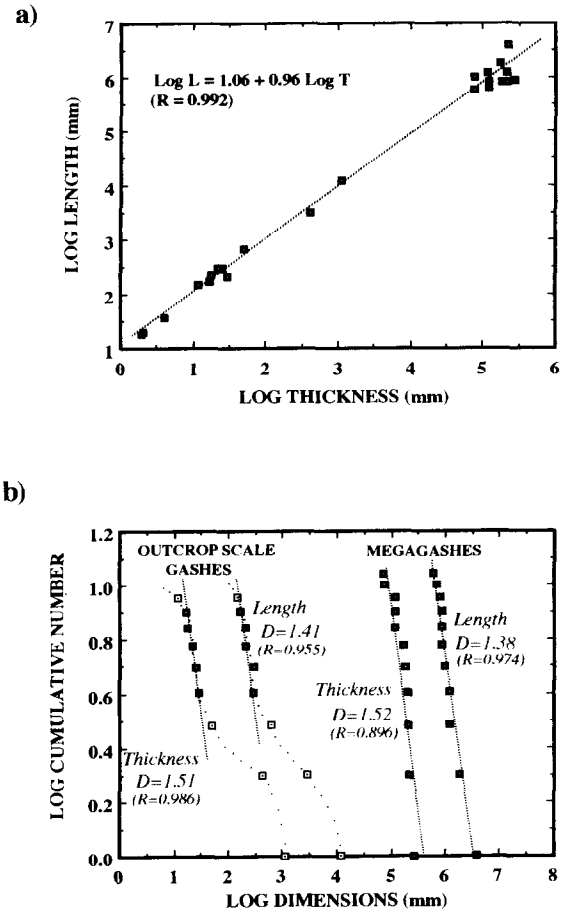

Fig. 10. (a) Plot of log length vs log thickness for gash veins of Cavalcante in a range of six orders of magnitude. Veins were measured in exposures/sections parallel to the transport direction and perpendicular to the shear plane. (b) Logarithimic plots of cumulative frequency for length and thickness. Because of the heterogeneous sampling, the gashes were plotted in two separated populations (outcrop and airphotograph scales). Slopes of the power-law segments in the two gash populations are similar, and indicate 'fractal dimensions' around 1.4 for length and 1.5 for thickness.

La Pointe, 1995) where for small veins $a < 1$, and for large veins $a > 1$. This kink in the power-law distribution was interpreted to reflect an abrupt change in the vein growth mechanism which causes a change in the aspect ratio of the veins above the critical thickness (Johnston and McCaffrey, 1996). On the other hand, a self-similar vein distribution with $a \sim 1$ along all vein size ranges, as occurs in the studied shear zone, indicates that opening and propagation of the gash fractures occurred simultaneously and with the same rates during vein formation, suggesting that a continuous process accounts for vein growth on all scales.

CONCLUSIONS

1. Kilometer-scale extension gashes developed during activation of the 20 km wide, continental-scale Cavalcante–Teresina shear zone, indicating a direct relationship between the magnitude/opening of tension fractures and the volume of deforming rock.
2. The occurrence of alternating zones of phyllonites and protomylonites (with extension gashes) within the Cavalcante–Teresina shear zone suggests that lateral compensation of volume occurred during deformation.
3. The amount of silica depleted in the phyllonite zones is approximately the same amount precipitated in the km-scale gash veins suggesting that the shear zone acted as a closed system for silica. Migration of silica from the phyllonites towards the extension gashes within the protomylonites should represent the main mechanism of lateral compensation of volume.
4. The km-scale extension gashes define the same power-law distribution as extension gashes of outcrop and microscale, indicating a wide range of scale-invariance for this phenomenon. The fractal set extends over six orders of magnitude with 'fractal dimensions' around 1.4 for vein length and 1.5 for vein thickness.
5. The aspect ratio of the gash veins does not change with scale ($a \sim 1$) reflecting a self-similar distribution where the same process should account for vein growth from micro- to km-scale.

Acknowledgements—Financial support for this research was provided by the Brazilian National Research Council (CNPq) and by the structural geology research program at the Geology Department (UFOP). Comments by J. Henderson, S. Marshak, C. Passchier, E. Tohver and two anonymous reviewers helped to improve the manuscript. We also thank M. Fonseca and Mineração Cavalcante S.A. for inviting us to work in this shear zone.

REFERENCES

Barton, C. and La Pointe, P. (1995) *Fractals in the Earth Sciences*. Plenum Press, New York.

Beach, A. (1975) The geometry of en-échelon vein arrays. *Tectonophysics* **28**, 245–263.

Blacic, J. (1975) Plastic deformation mechanisms in quartz: the effect of water. *Tectonophysics* **2**, 171–194.

Caby, R. and Arthaud, M. (1986) Major Precambrian nappes of the Brazilian belt, Ceará, northeast Brazil. *Geology* **14**, 871–874.

Caby, R., Sial, A. N., Arthaud, M. and Vauchez, A. (1991) Crustal evolution and the Brasiliano orogeny in Northeast Brazil. In *The West African Orogens and Circum Atlantic Correlatives*, ed. R. D. Dallmeyer and J. P. Lecorché, pp. 373–397. Springer, Berlin.

Cox, S., Wall, V., Etheridge, M. and Potter, T. (1991) Deformational and metamorphic processes in the formation of mesothermal vein-hosted gold deposits—examples from the Lachlan Fold Belt in central Victoria, Australia. *Ore Geology Reviews* **6**, 391–423.

Durney, D. (1981) Dilatancy and the angle of obliquity in en-échelon fractures. *Journal of the Geological Society of Australia* **4**, 38.

Engelder, T. (1987) Joints and shear fractures in rocks. In *Fracture Mechanics of Rock*, ed. B. K. Atkinson, pp. 27–65. Academic Press, London.

Fonseca, M. A. and Dardenne, M. A. (1993) Transcurrent fault systems in the north portion of the Brasília fold belt. In *II Simpósio do Craton do São Francisco, Salvador, Brasil, Abstract Volume*, pp. 280–282.

Fournier, R. and Potter, R. (1982) An equation correlating the solubility of quartz in water from 25 to 900° C at pressures up to 10,000 bars. *Geochimica et Cosmochimica Acta* **46,** 1969–1973.

Fueten, F., Robin, P.-Y. and Stephens, R. (1991) A model for the development of a domainal quartz *c*-axis fabric in a coarse-grained gneiss. *Journal of Structural Geology* **13,** 1111–1124.

Johnston, J. D. (1992) The fractal geometry of veins: potential for ore reserve calculations. In *The Irish Minerals Industry 1980–1990—A Review of the Decade, Galway 1990*, eds G. V. Earls, A. Bowdwn, P. O'Connor and J. Pyne, pp. 105–118. Irish Association for Economic Geology, Dublin.

Johnston, J. D. and McCaffrey, K. (1996) Fractal geometries of vein systems and the variation of scaling relationships with mechanism. *Journal of Structural Geology* **18,** 349–358.

Hancock, P. L. (1972) The analysis of en-échelon veins. *Geological Magazine* **109,** 269–276.

Hancock, P. L. (1985) Brittle microtectonics: principles and practice. *Journal of Structural Geology* **7,** 437–457.

Hippertt, J. (1994) Microstructures and *c*-axis fabrics indicative of quartz dissolution in sheared quartzites and phyllonites. *Tectonophysics* **229,** 141–163.

Mandelbrot, B. B. (1985) Self-affine fractals and fractal dimension. *Physica Scripta* **32,** 257–260.

Massucatto, A. J. and Hippertt, J. (1996) Gold mineralization associated with *S C* structures in kilometer-scale extension gashes: the example of Cavalcante, GO. In: 39 Congresso Brasileiro de Geologia, Sociedade Brasileira de Geologia, Salvador **Vol. 1,** 343–346.

Nicholson, R. (1991) Vein morphology, host rock deformation and the origin of the fabrics of echelon mineral veins. *Journal of Structural Geology* **13,** 635–641.

O'Hara, K. (1988) Fluid flow and volume loss during mylonitization: an origin for phyllonite in an overthrust setting, North Carolina, U.S.A. *Tectonophysics* **156,** 21–36.

O'Hara, K. and Blackburn, W. (1989) Volume-loss model for trace element enrichments in mylonites. *Geology* **17,** 524–527.

Ramsay, J. and Huber, M. (1987) *The Techniques of Modern Structural Geology, Volume 2: Folds and Fractures.* Academic Press, London.

Rickard, M. and Rixon, L. (1983) Stress configurations in conjugate quartz-veins arrays. *Journal of Structural Geology* **5,** 573–578.

Rothery, E. (1988) En-échelon vein array development in extension and shear. *Journal of Structural Geology* **10,** 63–71.

Selverstone, J., Morteani, G. and Staude, J.-M. (1991) Fluid channeling during ductile shearing: transformation of granodiorite into aluminous schist in the Tauern Window, Eastearn Alps. *Journal of Metamorphic Geology* **9,** 419–431.

Sibson, R. (1994) Crustal stress, faulting and fluid flow. In *Geofluids: Origin, Migration and Evolution of Fluids in Sedimentary Basins*, ed. J. Parnell, pp. 69–84. Geological Society of London Special Publication **78**.

Tullis, T. (1989) Development of preferred orientation due to anisotropic dissolution/growth rates during solution transfer creep. *Eos, Transactions of the American Geophysical Union* **70**(15), 457.

Vauchez, A., Neves, S., Caby, R., Corsini, M., Egydio-Silva, M., Arthaud, M. and Amaro, V. (1995) The Borborema shear zone system, NE Brazil. *Journal of South American Earth Sciences* **8,** 247–266.

Walsh, J. and Watterson, J. (1992) Populations of faults and fault displacements and their effects on estimates of fault-related regional extension. *Journal of Structural Geology* **14,** 701–712.